Progress in NMR Spectroscopy, Vol. 17, pp. 187–209, 1985.
Printed in Great Britain.

0079–6565/85/$0.00 + .50

MEASURING AND IMAGING OF FLOW BY NMR

JANEZ STEPIŠNIK
Physics Department, University E. Kardelj, 61000 Ljubljana, Jadranska 19, and Institute J. Stefan, Yugoslavia

(*Received* 1 *March* 1985)

CONTENTS

Preface	187
1. Spin Response	188
2. Spin Migration	192
3. Measurement of Flow Velocity	195
3.1. Magnetization transfer	195
3.2. Flow in an inhomogeneous rf field	196
3.3. Flow in a magnetic field gradient	198
4. Flow Imaging	202
4.1. Imaging by magnetization transfer	202
4.2. Flow phase encoding	202
4.3. Flow phase encoding by the spin warp technique	203
Appendix	206
References	208

PREFACE

The idea of using spins for measuring molecular migration dates back to the beginning of nuclear magnetic resonance (NMR). The potential of using NMR for studying either random microscopic flow (self-diffusion)[1–3] or macroscopic flow[4–10] was quickly realized. The major advantage of using NMR for these measurements is that the sample is unaffected by the measuring process since there is no direct contact with the fluid. Thus, from the very early days of NMR, flow measurements have been made on very different systems[11] which even included some physiological applications.[12,13] Several methods for measuring the spatial migration of spins have been proposed and most of them have been applied successfully.[14–19]

New techniques which allow us to determine the image of the spatial distribution of spins and their properties inside the macroscopic sample were first introduced in 1952.[20] NMR imaging was developed later[21–25] and used also for the visualization of the flow velocity distribution in a fluid. It allows us to measure the flow of fluids in a human body,[26–28] and provides diagnostic medicine[29] with important information about the functional assessment and physiological status of body organs.

NMR is quite sensitive to flow and to other kinds of spin migration and these affect almost all NMR images of parts of the human body. The number of NMR flow methods available for use is almost equal to the number of different imaging methods. The aim of this review is to consider systematically the parameters which reflect the effects of spin migration on NMR signals and to provide a classification of the different flow methods.

In spite of the fact that spin dynamics for flow and self-diffusion are usually described by modified phenomenological Bloch equations, the density matrix formalism is employed in this review. The advantage of this approach is that the expressions for the response of the spins to external magnetic and radiofrequency (rf) fields are more compact and allow the effect of spatial motion to be visualized more clearly.

1. SPIN RESPONSE

The free energy change of a coil containing a sample of magnetic moment $\mathbf{M}$ at constant temperature produced by a change in magnetic field δB_1 is

$$\delta F = -\mathbf{M}\delta B_1, \tag{1}$$

where B_1 is the magnetic field at the location of the magnetic moment. The free energy can be also expressed in terms of an electric current i_c which produces a field B_1, and a magnetic flux ϕ induced by the magnetic moment of the sample

$$\delta F = -\phi\delta i_c. \tag{2}$$

Thus, U the voltage induced in the coil[30] is

$$U = -\frac{\mathrm{d}\phi}{\mathrm{d}t} = \frac{\mathrm{d}}{\mathrm{d}t}\frac{\delta F}{\delta i_c} = -\frac{\mathrm{d}}{\mathrm{d}t}\left(\mathbf{M}\frac{\delta B_1}{\delta i_c}\right). \tag{3}$$

To distinguish between the magnetic fields in the receiver and transmitter coils, that of the receiver coil will be denoted as B_{1r}, while the magnetic field of the transmitter coil is given as B_{1t}. In a sample with many microscopic magnetic moments (the spins), the induced emf is given by

$$U = -\frac{\hbar\gamma}{i_c}\frac{\mathrm{d}}{\mathrm{d}t}\sum_j \langle B_{1r}(\mathbf{r}_j)I_{yj}\rangle, \tag{4}$$

where γ is the magnetogyric ratio and $\mathbf{r}_j$ is the radius vector of the location of the jth spin; I_{yj} is the component of the spin operator along the coil axis. Expression (4) shows that if a coil carrying a unit current produces a field B_{1r} at the point of a spin then the rotating magnetic dipole of the same spin induces in that coil an emf proportional to the sum of the products between the spins and their related magnetic fields. The average can be evaluated using the density matrix operator $\rho(t)$ to give

$$U = \frac{\hbar}{i_c}\frac{\mathrm{d}}{\mathrm{d}t}\sum_j \mathrm{Tr}\,\rho(t)\omega_{1r}(\mathbf{r}_j)I_{yj}, \tag{5}$$

where $\omega_{1r} = \gamma B_{1r}$.

By using the time evolution operator $U(t)$ the density matrix can be formally written as

$$\rho(t) = U(t)\rho(0)U^{-1}(t), \tag{6}$$

where $\rho(0)$ is the initial density matrix at the moment when spin excitation starts. In the high temperature approximation the equilibrium density matrix is

$$\rho(0) = \rho_L\left(1 - \hbar\omega_0\sum_j \mathscr{B}_j I_{zj}\right), \tag{7}$$

where the matrix operator of the lattice is ρ_L and where $\mathscr{B}_j$ describes the degree of spin longitudinal magnetization. The longitudinal magnetization of spins may be non-uniform either due to an inhomogeneous static magnetic field or due to some perturbation prior to the experiment, and thus $\mathscr{B}_j$ depends upon the location of spins. An example is flow measurements made by the time-of-flight method, where $\mathscr{B}_j$ depends upon the time which the spins spend in the magnet.

The time evolution operator in the expression (6) is defined with the hamiltonian by the formal relation

$$U(t) = T\exp\left(-i\int_0^t \mathscr{H}(t')\,\mathrm{d}t'\right). \tag{8}$$

The time ordering operator T prevents direct evaluation of eqn. (8) by simple integration of the commulant and it is necessary to employ some approximate techniques.

The general objective of the flow measuring techniques is to label the spins in some manner. In magnetic resonance this is achieved by applying a non-uniform magnetic field. If the static magnetic field B_0 is inhomogeneous along the sample, then the precessional angular frequency ω_0 of the spins

$$\omega_0 = \gamma B_0 \tag{9}$$

depends upon the spin location as well as the spin magnetization. Thus the spatial displacement is shown as a frequency displacement. A similar effect can be achieved by a non-uniform field of the transmitter or receiver coil. If the rf field of the transmitter coil B_{1t} is non-uniform, the degree of spin excitation depends upon the spin location and if the field B_{1r} is non-uniform the receiver coil detects signals which also depend upon spin location.

In practice a non-uniform magnetic field is achieved by employing a non-uniform magnetic field in addition to the static uniform field B_0. According to Maxwell's equations, a non-uniform magnetic field has always more than one component different from zero. Therefore, if an additional field is weak enough the total magnetic field can be written as

$$B = B_0 + \mathcal{G}\mathbf{r}, \tag{10}$$

where $\mathcal{G}$ is a tensor.[28] The parts of the hamiltonian which include the interactions with the magnetic field components perpendicular to the magnetic field B_0 do not commute with the main part which includes B_0. Thus in the case that the additional field is changing at a slower rate than the inverse larmor frequency, the perpendicular components of the magnetic field from the expression (10) can be discarded and the magnetic field approximated as

$$B = B_0 + \mathbf{G}\mathbf{r}, \tag{11}$$

where $\mathbf{G}$ is the gradient of the component parallel to the main field. The gradient can be either static or time dependent which means that its magnitude and direction can both be changing.

The rf transmitter coil generates a magnetic field

$$B'_{1t} = B_{1t}(\mathbf{r}_1 t)\sin\omega_0 t \tag{12}$$

which excites the spins. In a selective excitation experiment where only the magnetization in a thin slice of the sample precesses in a transverse plane the magnetic field gradient is applied during the rf irradiation period. Thus only spins in a certain plane are at exact resonance and interact strongly with the rf pulse. The shape of the rf pulses is not rectangular but is modulated with the desired spectral distribution. Thus the magnitude of the rf excitation pulse is a function of time and position in general.

Here it is assumed that the hamiltonian describing the system, and the spin dynamics in particular, consists of four parts

$$\mathcal{H}(t) = \mathcal{H}_z + \mathcal{H}_G(t) + \mathcal{H}_{rf}(t) + \mathcal{H}_L. \tag{13}$$

The Zeeman part

$$\mathcal{H}_z = -\hbar\omega_0 \sum_j I_{zj}, \tag{14}$$

the gradient part

$$\mathcal{H}_G(t) = -\hbar\gamma\mathbf{G}(t)\sum_j(\mathbf{r}_j - \mathbf{r}_0)I_{zj}, \tag{15}$$

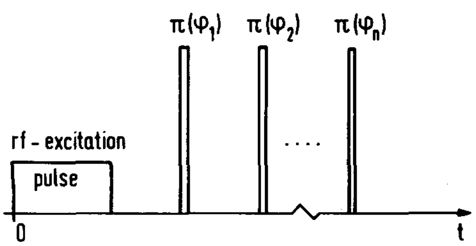

FIG. 1. The basic spin echo rf pulse sequence.

the radiofrequency part

$$\mathscr{H}_{\mathrm{rf}}(t) = -\hbar \sum_j \omega_{1\mathrm{t}}(\mathbf{r}_j, t) \sin(\omega_0 t + \delta) I_{xj}, \tag{16}$$

and the hamiltonian $\mathscr{H}_{\mathrm{L}}$, which includes all the remaining static interactions such as the spin–spin interaction, as well as time dependent interactions both between spins and with the lattice.

In the ordinary NMR free precession experiment only the excitation rf pulse is applied. Here we shall consider a more general approach where the spin excitation is achieved using a type of spin–echo rf pulse sequence consisting of a $\pi/2$ pulse and a sequence of π pulses of various phases (Fig. 1). In contrast to the initial excitation pulse whose magnitude depends upon the spin location, the field $B_{1\mathrm{t}}$ of the π rf pulses is assumed to be completely uniform. In order to simplify further consideration the π pulses are assumed to be short enough to neglect their spatial selectivity when applied simultaneously with the magnetic gradient.

Here we shall adopt a treatment of the spins which uses a time evolution operator written as a product[31]

$$U(t) = U_{\mathrm{L}} U_z U_{\mathrm{rf}\pi} U_{\mathrm{G}} U_{\mathrm{rfe}}, \tag{17}$$

where U_{L} includes only the hamiltonian $\mathscr{H}_{\mathrm{L}}$, U_z is the part due to the Zeeman interactions, $U_{\mathrm{rf}\pi}$ is from the interactions with the π pulses, U_{G} is related to the gradient interactions and U_{rfe} represents the spin time evolution due to excitation by the initial rf pulse. Each separation of the time evolution operator means that the transformation is in a new interaction representation. Thus, by removing the Zeeman part by the operator

$$U_z(t) = \exp(-i\mathscr{H}_z t), \tag{18}$$

the remaining hamiltonian is transformed into the frame rotating around the z-axis with the free precession frequency ω_0. By separating off the π part with the operator

$$U_{\mathrm{rf}\pi} = T \exp\left(-i \int_{\tau}^{t} \tilde{\mathscr{H}}_{\mathrm{rf}\pi}(t')\,\mathrm{d}t' \right) \tag{19}$$

with

$$\tilde{\mathscr{H}}_{\mathrm{rf}\pi}(t) = U_z^{-1} U_{\mathrm{L}}^{-1} \mathscr{H}_{\mathrm{rf}\pi}(t) U_{\mathrm{L}} U_z \tag{20}$$

the system is transformed into a tilted frame. By separating the time evolution operator of the gradient field with

$$U_{\mathrm{G}} = \exp\left(-i \int_{0}^{t} \tilde{\mathscr{H}}_{\mathrm{G}}(t')\,\mathrm{d}t' \right), \tag{21}$$

with

$$\begin{aligned} \tilde{\mathscr{H}}_{\mathrm{G}}(t) &= U_{\mathrm{rf}\pi}^{-1} U_{\mathrm{L}}^{-1} \mathscr{H}_{\mathrm{G}}(t) U_{\mathrm{L}} U_{\mathrm{rf}\pi} \\ &= -\gamma\hbar \mathbf{G}_{\mathrm{eff}}(t) \sum_j (\mathbf{r}_j(t) - \mathbf{r}_0) I_{zj}, \end{aligned} \tag{22}$$

one performs the transformation into a non-uniformly rotating frame which rotates with the frequency determined by the effective magnetic field gradient. The effective gradient is the magnetic gradient transformed by $U_{\mathrm{rf}\pi}$ into a tilted frame (22). After all these transformations the remaining rf excitation operator

$$U_{\mathrm{rfe}} = T \exp\left(-i \int_{0}^{\tau} \tilde{\mathscr{H}}_{\mathrm{rfe}}(t')\,\mathrm{d}t' \right) \tag{23}$$

includes the transformed hamiltonian

$$\tilde{\mathscr{H}}_{\mathrm{rfe}}(t) = U_{\mathrm{G}}^{-1} U_z^{-1} U_{\mathrm{L}}^{-1} \mathscr{H}_{\mathrm{rf}}(t) U_{\mathrm{L}} U_z U_{\mathrm{G}}. \tag{24}$$

Substitution of the expressions (18)–(23) into eqn. (5) gives the voltage as

$$U = \frac{\hbar^2\omega_0}{i_c}\frac{\mathrm{d}}{\mathrm{d}t}\sum_{ji}\langle Tr U_L U_z U_{\mathrm{rf}\pi} U_G U_{\mathrm{rfe}} I_{zi} U_{\mathrm{rfe}}^{-1} U_G^{-1} U_{\mathrm{rf}\pi}^{-1} U_z^{-1} U_L^{-1} I_{yj}\omega_{1r}(\mathbf{r}_j(t))\rangle_L \mathscr{B}_i. \tag{25}$$

Here the bracket $\langle\ \rangle_L$ represents the average over all other degrees of freedom except that of the spin. The purpose of the initial excitation rf pulse is to transform longitudinal into transverse magnetization either in the whole volume of the sample or in a certain selected part. In order to achieve a selective excitation, the rf pulse is applied simultaneously with the magnetic field gradient. The effect of such combined excitation on the spin system has been treated using different approaches.[28] In the Appendix both exact and approximative calculations are given but in the following it will be expressed in general form as

$$U_{\mathrm{rfe}} I_{zj} U_{\mathrm{rfe}}^{-1} = A_j(t) I_{xj} + B_j(t) I_{yj} + C_j(t) I_{zj}. \tag{26}$$

The further evaluation with the gradient term gives

$$U_G U_{\mathrm{rfe}} I_{zj} U_{\mathrm{rfe}}^{-1} U_G^{-1} = M(\mathbf{r}_j)[I_{xj}\cos(\varphi_j(t)+\alpha_j) + I_{yj}\sin(\varphi_j(t)+\alpha_j)] + C_j I_{zj} \tag{27}$$

with

$$M(\mathbf{r}_j) = \sqrt{A_j^2(t) + B_j^2(t)} \tag{28}$$

and

$$\alpha_j = \tan^{-1}\frac{A_j(t)}{B_j(t)} \tag{29}$$

and where

$$\varphi_j(t) = \gamma\int_0^t \mathbf{G}_{\mathrm{eff}}(t')[\mathbf{r}_j(t') - \mathbf{r}_0]\,\mathrm{d}t'. \tag{30}$$

Transformation into the tilted frame by $U_{\mathrm{rf}\pi}$ changes the sign of the operator I_{zj}. It also changes the sign either of I_{xj} or I_{yj} depending upon the phase of the π pulses and on the number of pulses before the time of measurement. In general we denote the sign of I_{xj} as $P_x(t)$ and of I_{yj} as $P_y(t)$ at the time t. By substitution of eqn. (27) into eqn. (25) we get

$$\begin{aligned} U I_{zj} U^{-1} = M(\mathbf{r}_j)[&P_x I_{xj}\cos\omega_o t\cos[\varphi_j(t)+\alpha_j] - P_y I_{xj}\sin\omega_0 t\sin[\varphi_j(t)+\alpha_j] \\ &+ P_x I_{yj}\sin\omega_0 t\cos[\varphi_j(t)+\alpha_j] + P_y I_{yj}\cos\omega_0 t\sin[\varphi_j(t)+\alpha_j]] + P_x P_y C_j I_{zj}. \end{aligned} \tag{31}$$

Taking the derivative with time in the expression (25), the emf induced in the receiver coil becomes

$$U = \frac{\hbar^2\omega_0^2}{i_c} P_x \sum_j \mathscr{B}_j Tr\, I_{xj} I_{xj}(t)\langle M(\mathbf{r}_j(0))\omega_{1r}(\mathbf{r}_j(t))\cos[\varphi_j(t)+\alpha_j+P_x P_y\omega_0 t]\rangle_L. \tag{32}$$

In taking the time derivative all other modulations, except the free precession with an averaged frequency ω_0 have been neglected. It is assumed that the system is in a strong Zeeman magnetic field and that all other spin interactions are small perturbations.

Equation (32) represents the basic expression for the spin response in the case of measuring or imaging flow, and the effects of spin migration are determined by the parameters in this expression. The parameter $\mathscr{B}_j$ is proportional to the longitudinal magnetization, and depends upon the velocity at which the inflowing spins have insufficient time to reach the equilibrium value $\mathscr{B}_0$. In the saturation recovery sequence $\mathscr{B}$ depends upon the repetition time t_R between successive excitations, so that

$$\mathscr{B} = \mathscr{B}_0\left(1 - \exp\left(-\frac{t_R}{T_1}\right)\right), \tag{33}$$

where T_1 is the longitudinal relaxation time. In the inversion recovery sequence or under the condition of adiabatic fast passage, where the magnetization has been reversed prior to the excitation, it behaves as

$$\mathscr{B} = \mathscr{B}_0\left(1 - 2\exp\left(-\frac{t_R}{T_1}\right)\right). \tag{34}$$

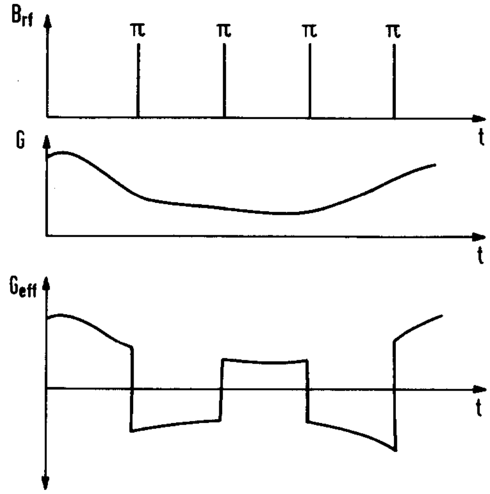

FIG. 2. The shaping of the effective magnetic field gradient, G_{eff}, by π pulses.

The parameter $Tr\, I_{xj}(t) I_{xj}(0)$ describes the spin–spin interactions. It modulates the free precession signal with additional frequencies depending upon the internal magnetic fields created by neighbouring spins. In high resolution spectroscopy it produces a number of lines belonging to chemically non-equivalent spins. Here the spin–spin interactions will be described only by the relaxation time T_2 *as*

$$Tr\, I_{xj} I_{xj}(t) = Tr\, I_{xj}^2 \exp\left(-\frac{t}{T_2}\right). \tag{35}$$

The parameter $M(\mathbf{r}_j)$ in eqn. (32) becomes independent of the spin location when there is no magnetic field gradient and when B_{1t} is uniform along the sample

$$M = \sin\left(\gamma \int_0^{\tau} B_{1t}(t)\,\mathrm{d}t\right). \tag{36}$$

Under the same condition the phase α is zero.

In the ordinary free induction decay experiment in the absence of any π rf pulses, P_x and P_y are equal to unity, but in spin–echo experiments which use a sequence of π pulses their values may be $+1$ or -1, leading to a change in the sign of the signal and the sign of the phase. But the π rf pulses have a more significant effect on the magnetic field gradient. After each π pulse the sign of the gradient is reversed (Fig. 2), so that the effective gradient can be written as

$$\mathbf{G}_{eff}(t) = P_x(t) P_y(t) \mathbf{G}(t). \tag{37}$$

2. SPIN MIGRATION

The radius vector of the migrating spin $\mathbf{r}_j$ changes with time. An averaged spin location can be expressed simply as

$$\langle \mathbf{r}_j(t) \rangle = \mathbf{r}_{j0} + \mathbf{v}_j t, \tag{38}$$

where $\mathbf{v}_j$ is the averaged velocity vector of jth spin during acquisition time of the FID in the NMR experiment. In the spin response given by eqn. (32) the migration affects the receiving ability of the coil through the parameter $\omega_{1r}(\mathbf{r}_j(t))$ and also changes the phase

$$\varphi_j(t) = \gamma \int_0^t \mathbf{G}_{eff}(t')\,(\mathbf{r}_j(t') - \mathbf{r}_0)\,\mathrm{d}t'.$$

The detailed treatment of the effect caused by variations in ω_{1r} is given in Section 3.2 where an FID in a non-uniform rf field is considered. Here only effects caused by motion of the spins through the magnetic field gradient will be considered. Neglecting the rf non-uniformity then the average only of

$$\langle \cos(\varphi_j(t)+\alpha_j)\rangle_{\mathrm{L}} \tag{39}$$

needs to be evaluated. This can be done using the commulant expansion theorem.[32] If only the first two terms of the expansion are taken into account[33] the expression (39) is transformed into

$$\langle \cos(\varphi_j(t)+\alpha_j)\rangle_{\mathrm{L}} = \exp(-\xi(t))\cos(\langle\varphi_j(t)\rangle_{\mathrm{L}}+\alpha_j), \tag{40}$$

where

$$\xi(t) = \frac{\gamma^2}{2}\int_0^t \mathrm{d}t_1 \int_0^t \mathrm{d}t_2 \mathbf{G}_{\mathrm{eff}}(t_1)\langle \mathbf{r}_j(t_1)\mathbf{r}_j(t_2)\rangle_{\mathrm{LC}}\mathbf{G}_{\mathrm{eff}}(t_2), \tag{41}$$

with

$$\langle \mathbf{r}_j\mathbf{r}_j\rangle_{\mathrm{LC}} = \langle \mathbf{r}_j\mathbf{r}_j\rangle_{\mathrm{L}} - \langle \mathbf{r}_j\rangle_{\mathrm{L}}\langle \mathbf{r}_j\rangle_{\mathrm{L}}, \tag{42}$$

and

$$\langle \varphi_j(t)\rangle_{\mathrm{L}} = (\mathbf{r}_{j0}-\mathbf{r}_0)\mathbf{F}(t)+\mathbf{v}_j\mathbf{f}(t), \tag{43}$$

with

$$\mathbf{F}(t) = \gamma \int_0^t \mathbf{G}_{\mathrm{eff}}(t')\,\mathrm{d}t', \tag{44}$$

and

$$\mathbf{f}(t) = \gamma \int_0^t t' G_{\mathrm{eff}}(t')\,\mathrm{d}t'. \tag{45}$$

The expression (40) represents an attenuated oscillation, with the attenuation determined by the parameter $\xi(t)$, which depends upon the spin coordinates at different times and is related to the randomization of spins caused by migration since it arises from turbulent flow or microscopic self-diffusion. Applying a gradient along the x-axis, $\xi(t)$ becomes

$$\xi(t) = \frac{\gamma^2}{2}\int_0^t \mathrm{d}t_1 \int_0^t \mathrm{d}t_2 G_{x\,\mathrm{eff}}(t_1)G_{x\,\mathrm{eff}}(t_2)\langle x_j(t_1)x_j(t_2)\rangle_{\mathrm{LC}}, \tag{46}$$

where location correlation can be expressed by the velocity autocorrelation function

$$\langle x_j(t_1)x_j(t_2)\rangle_{\mathrm{LC}} = \frac{1}{\pi}\int_{-\infty}^{\infty} D_{xx}(\omega)\frac{\exp(i\omega(t_1-t_2))}{\omega^2}\,\mathrm{d}\omega, \tag{47}$$

where $D_{xx}(\omega)$ is the spectrum of the x-component of the velocity correlation:

$$D_{xx}(\omega) = \int_0^{\infty} \langle v_{xj}(0)v_{xj}(t)\rangle_{\mathrm{L}}\, \mathrm{e}^{i\omega t}\,\mathrm{d}t. \tag{48}$$

$D_{xx}(0)$, the value at $\omega = 0$, is identical to the self-diffusion coefficient, D. If the spectrum of the magnetic field gradient is defined as

$$G(\omega_1 t) = \int_0^t G_{x\,\mathrm{eff}}(t')\exp(i\omega t')\,\mathrm{d}t', \tag{49}$$

then by substitution of eqns (47)–(49) into eqn. (46) the attenuation parameter becomes

$$\xi(t) = \frac{\gamma^2}{2\pi}\int_{-\infty}^{\infty} \frac{D_{xx}(\omega)}{\omega^2}|G(\omega,t)|^2\,\mathrm{d}\omega. \tag{50}$$

This is the convolution between the spectrum of the velocity autocorrelations and the spectrum of the effective gradient (Fig. 3).

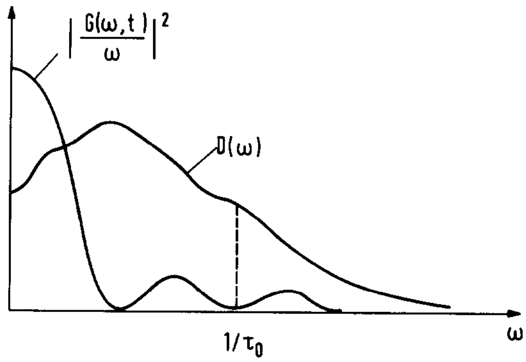

FIG. 3. The convolution between the spectrum of velocity autocorrelations, $D(\omega)$, and the spectrum of the effective field gradient.

Whenever the correlation time of the molecular dynamical processes, τ_0, is short compared to the time scale of the NMR measurement only the low frequency part of $D_{xx}(\omega)$ plays a role in eqn. (49). In this case $\xi(t)$ can be approximated to

$$\xi(t) \cong \frac{\gamma^2}{2\pi} D_{xx}(0) \int_{-\infty}^{\infty} \frac{|G(\omega_1 t)|^2}{\omega^2} \mathrm{d}\omega, \tag{51}$$

which is equivalent to the well-known result derived by Torrey[3] for spin–echo damping, if the Parceval identity is taken into account,

$$\xi(t) \cong \gamma^2 D_{xx}(0) \int_0^t \left| \int_0^u G_{x\,\mathrm{eff}}(t')\,\mathrm{d}t' \right|^2 \mathrm{d}u. \tag{52}$$

This means that eqn. (52) is just an approximation of the more general expression (50) which is also valid for long correlation times, especially when the dynamics of turbulent flow are considered. Thus, the measurement of self-diffusion by NMR might also yield information about the velocity autocorrelations, i.e. its spectrum.

By replacing eqns (35) and (40) in eqn. (32) the emf of the receiver coil is

$$U = \frac{\hbar^2\omega_0^2}{i_c} P_x \sum_j \mathscr{B}_j M(\mathbf{r}_{j0})\, Tr\ I_{xj}^2 \exp\left(-\frac{t}{T_{2j}} - \xi_j(t)\right)$$
$$\times\, \omega_1(\mathbf{r}_{j0} + \mathbf{v}_j t) \cos[\mathbf{F}(t)(\mathbf{r}_{j0} - \mathbf{r}_0) - \mathbf{f}(t)\mathbf{v}_j + \alpha_j + P_x P_y \omega_0 t], \tag{53}$$

which can be written in the continuum limit as

$$U = \frac{\hbar^2\omega_0^2}{i_c} P_x Tr\, I_{xj}^2 \int \mathrm{d}^3 r \mathscr{B}(\mathbf{r}) M(\mathbf{r}) \rho(\mathbf{r}) \exp\left(-\frac{t}{T_2(\mathbf{r})} - \xi(\mathbf{r}, t)\right)$$
$$\times\, \omega_1(\mathbf{r} + \mathbf{v}(\mathbf{r})t) \cos[\mathbf{F}(t)(\mathbf{r} - \mathbf{r}_0) + \mathbf{f}(t)\mathbf{v}(\mathbf{r}) + \alpha(\mathbf{r}) + P_x P_y \omega_0 t]. \tag{54}$$

Here the spin density is defined as

$$\rho(\mathbf{r}) = \sum_j \delta(\mathbf{r} - \mathbf{r}_{j0}), \tag{55}$$

and $Tr\, I_{xj}^2$ means the trace over one spin.

In eqns (53) and (54) B_{1t} of the π pulses is assumed to be uniform in the excited part of the sample. This means that the active region of the transmitter coil should be larger than the width of the selected slice, and spin migration should be slow enough to avoid an appreciable outflow of spins from the coil in the time of acquisition of the FID. These restrictions are related only to the π refocusing pulses; the magnitude of the initial rf pulse may be non-uniform along the sample. A detailed analysis of the case of spin refocusing by non-uniform π pulses gives a spin response which is much more complicated than eqn. (54). Such a case is treated later by considering a spin–echo experiment on a flowing liquid. However, with the restriction discussed above, eqn. (53) is a general description of the spin response of the fluid. There are various parameters dependent upon the flow velocity which can play the dominant role in any particular chosen experimental procedure.

In the NMR imaging experiment the emf signal given by eqn. (54) is converted into a free induction signal by two phase sensitive demodulators. This gives two signals U_{d1} and U_{d2} which can be written in complex form as

$$U_D = U_{d1} + U_{d2} = K \int \rho_{eff}(\mathbf{r}_1 \mathbf{v}_1 t) M(\mathbf{r}) \exp\{i[\mathbf{F}(t)(\mathbf{r}-\mathbf{r}_0) + \mathbf{f}(t)\mathbf{v}(\mathbf{r}) + \alpha(\mathbf{r})]\} \, d^3 r, \tag{56}$$

with

$$K = \frac{\hbar^2 \omega_0^2}{i_c} Tr\, I_{xj}^2 \tag{57}$$

and

$$\rho_{eff}(\mathbf{r}, \mathbf{v}, t) = \mathscr{B}(\mathbf{r}) \omega_{1r}(\mathbf{r} + \mathbf{v}(\mathbf{r})t) \rho(\mathbf{r}) \exp\left(-\frac{t}{T_2(\mathbf{r})} - \xi(\mathbf{r}, t) \right). \tag{58}$$

This expression, which is applicable to various imaging schemes after Fourier transformation, gives us information about the distribution of spin density, the distribution of relaxation times T_1 and T_2 and also information about random flow $\xi(t)$ or the velocity distribution of the flow. The velocity distribution can be obtained either from incomplete magnetization recovery or transfer of magnetization from $\mathscr{B}$, the effects due to the rf field non-uniformity seen in ω_{1r} and $M(\mathbf{r})$, or are found from the phase changes $\exp(i\mathbf{f}\mathbf{v})$. These particular cases will be considered in detail later in this review.

3. MEASUREMENT OF FLOW VELOCITY

3.1. *Magnetization Transfer*

The parameter $\mathscr{B}$ in eqn. (54) is a measure of the amount of spin longitudinal magnetization. It is also called the spin temperature. In the static magnetic field in the absence of an rf field, $\mathscr{B}$ approaches its equilibrium value as

$$\frac{d}{dt}\mathscr{B} = \frac{\mathscr{B}_0 - \mathscr{B}}{T_1}, \tag{59}$$

where $\mathscr{B}_0$ is determined by the static magnetic field B_0. In eqn. (54) the parameter $\mathscr{B}(r)$ is the magnetization at the moment of spin excitation, i.e. at the time when the first rf pulse is applied. Its spatial distribution may depend upon the history of the sample. For example, if prior to the observation, the spins in the flowing fluid had been saturated by an rf pulse then after a time which is shorter than T_1, fresh spins, unaffected by the saturating pulse, enter the active region, then $\mathscr{B}$ is proportional to the velocity distribution (Fig. 4), $\mathscr{B}(r) \approx v(r)$.[9,17,34]

In the time-of-flight method[9] the transfer of magnetization between two coils is used for the determination of the flow velocity. The first coil labels the spins and the second coil detects their time of flight (Fig. 5). In these two examples, the spins have sufficient time to become fully polarized before entering the coils. Some earlier techniques for flow measurement[9] used the effect of incomplete spin

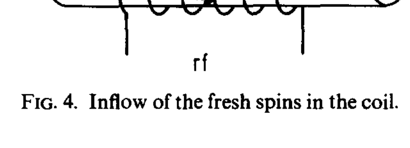

FIG. 4. Inflow of the fresh spins in the coil.

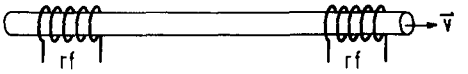

FIG. 5. The arrangement of the coils in the measurement of flow by the time-of-flight method.

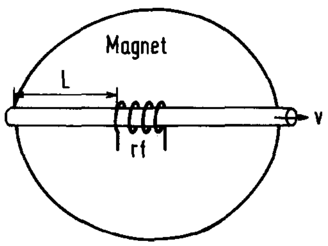

FIG. 6. The position of the coil in the magnet in flow measurement by the method of incomplete magnetization.

magnetization. If the spin path from the entrance of the magnet to the rf coil is L (Fig. 6), then

$$\mathscr{B} = \mathscr{B}_0\left(1 - \exp\left(-\frac{L}{vT_1}\right)\right). \tag{60}$$

Using more sophisticated rf pulse sequences the same effects can be observed in a different situation. Since this has been reviewed by Jones and Child,[34] more attention will be paid to other parameters of the flow which affect the NMR signal.

3.2. *Flow in an Inhomogeneous rf Field*

The rf field non-uniformity along the sample, which affects the parameter $\omega_{1r}(\mathbf{r}_j(t))$ for the receiver coil and $M(\mathbf{r}_j)$ for the transmitter coil, plays a role in almost any flow experiment,[45] because any finite length of the coil provides a kind of rf field inhomogenity. Here we shall consider the effects of the flow where only the spatial dependence of the rf field is involved, assuming that the spins are completely polarized before entering the coil and that there is no magnetic field gradient. Thus eqn. (32) can be reduced to

$$U = \frac{\hbar^2\omega_0^2}{i_c}\mathscr{B}_0 \sum_j Tr\, I_{xj} I_x(t) \langle \omega_{1r}(\mathbf{r}_j(t)) M(\mathbf{r}_j(0)) \rangle_L \cos\omega_0 t, \tag{61}$$

where

$$M(\mathbf{r}_j(0)) = \sin\left[\int_0^t \omega_{1t}(\mathbf{r}_j(t'), t')\,\mathrm{d}t'\right] \tag{62}$$

and

$$\omega_{1t} = \gamma B_{1t}(\mathbf{r}_j(t), t). \tag{63}$$

B_{1t} is the magnitude of the transverse magnetic flux density in the transmitter coil. The spatial dependence of $\omega_{1r}(\mathbf{r}_j(t))$ and $M(\mathbf{r}_j(0))$ can be expanded as

$$\omega_{1r}(\mathbf{r}_j) = \frac{1}{2\pi}\int_{-\infty}^{\infty} \omega_{1r}(\mathbf{q}) \exp[i\mathbf{q}\mathbf{r}_j]\,\mathrm{d}^3q, \tag{64}$$

and

$$M(\mathbf{r}_j) = \frac{1}{2\pi}\int_{-\infty}^{\infty} M(\mathbf{q}) \exp[i\mathbf{q}\mathbf{r}_j]\,\mathrm{d}^3q. \tag{65}$$

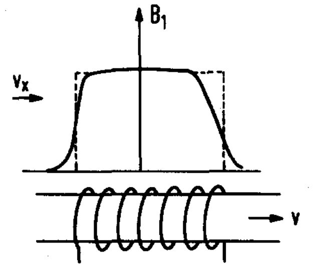

FIG. 7. Inhomogeneity of the rf field produced by a solenoidal coil.

By substitution of eqns (64) and (65) into eqn. (61) and assuming that the spin–spin interactions described by the relaxation time T_2, are uniform along the sample, one obtains

$$U = \frac{\hbar^2\omega_0^2}{4\pi i_c}\mathscr{B}_0 \int d^3q\, d^3q'\omega_{1r}(\mathbf{q})M(\mathbf{q}')\sum_j \langle \exp[i\mathbf{q}\mathbf{r}_j(t)+i\mathbf{q}\mathbf{r}_j(0)]\rangle_L \, Tr\, I_x^2 \exp\left[-\frac{t}{T_2}\right]\cos\omega_0 t. \quad (66)$$

The average of the exponential function in eqn. (66) can be expressed to the second order of approximation by the commulant expansion[32]

$$\langle \exp[i\mathbf{q}\mathbf{r}(t)+i\mathbf{q}\mathbf{r}(0)]\rangle_L = \exp[i\mathbf{q}\langle\mathbf{r}(t)\rangle_L + \mathbf{q}'\langle\mathbf{r}(0)\rangle_L - \tfrac{1}{2}\mathbf{q}\langle\mathbf{r}(t)\mathbf{r}(0)\rangle_{LC}\mathbf{q}'t. \quad (67)$$

By assuming eqn. (38) and that

$$\langle\mathbf{r}(t)\mathbf{r}(0)\rangle_{LC} = 2\underset{\sim}{D}t \quad (68)$$

and that the spin density is uniform then

$$U = \frac{\hbar^2\omega_0^2}{2\pi i_c}\mathscr{B}_0\, Tr\, I_x^2\cos(\omega_0 t)\int \omega_{1r}(\mathbf{q})M(-\mathbf{q})\exp\left[-\frac{t}{T_2} - \mathbf{q}\underset{\sim}{D}\mathbf{q}t + i\mathbf{q}\mathbf{v}t\right]d^3\mathbf{q}. \quad (69)$$

This is valid only for plug flow where the velocity is independent of spin location. In eqn. (69) an additional damping appears which is due to molecular self-diffusion, D, and the phase shift caused by the flow velocity, $\mathbf{v}$.[35]

In the case where the rf field distribution of the transmitter/receiver coil system is uniform within the length of the coil and zero outside it (Fig. 7) and with the direction of flow along the coil, then the free induction signal is

$$U = \frac{\hbar^2\omega_0^2}{i_c}S\mathscr{B}_0\, Tr\, I_x^2\cos(\omega_0 t)\exp\left[-\frac{t}{T_2}\right]\omega_{1r}M(l-vt). \quad (70)$$

The spin outflow from the active region of the coil brings about an additional reduction of the signal and which is described by the factor $(l-vt)$ in eqn. (70).

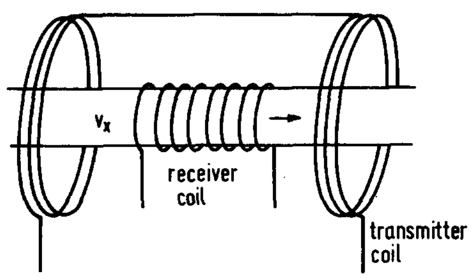

FIG. 8. The arrangement of transmitter and receiver coils in flow measurement by the method using a linear gradient of the transmitter rf field.

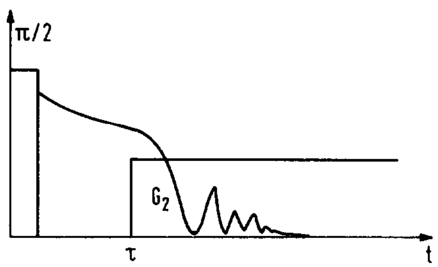

FIG. 9. The oscillations in the FID produced by a flowing sample in a magnetic field gradient.

The next example is a transmitter coil which produces an rf field with an almost constant field gradient along the sample

$$B_{1t} = \mathbf{G}_t(\mathbf{r}-\mathbf{r}_0). \tag{71}$$

This is produced by a reversed Helmholtz coil (Fig. 8). The receiver coil is usually a solenoid with a uniform rf field within the length of the coil. Equation (62) gives

$$M(q) = i\pi[\delta(q+q_0)\exp(-iq_0x_0)-\delta(q-q_0)\exp(iq_0x_0)], \tag{72}$$

where

$$q_0 = \gamma \int_0^\tau G_{xt}(t)\,dt, \tag{73}$$

and from eqn. (66),

$$U = 2\frac{\hbar\omega_0^2}{i_c q_0} S\mathscr{B}_0\, Tr\, I_x^2 \cos\omega_0 t \exp\left[-\left(\frac{1}{T}+q_0 D q_0\right)t\right]\sin q_0\frac{l}{2}\sin q_0(vt-r_0). \tag{74}$$

Thus, the emf in the receiver coil is modulated by the frequency $q_0 v$ and attenuated by $q_0 D q_0$ in addition to the attenuation by the normal T_2 decay. Here S is the sample cross-section.

3.3. *Flow in a Magnetic Field Gradient*

In the simplest case the sample is excited by a $\pi/2$ rf pulse followed later by a gradient of the magnetic field along the receiver coil axis, G_z. The emf is recorded during the time that the gradient is turned on (Fig. 9). Neglecting self-diffusion and assuming complete magnetization and uniform spin-

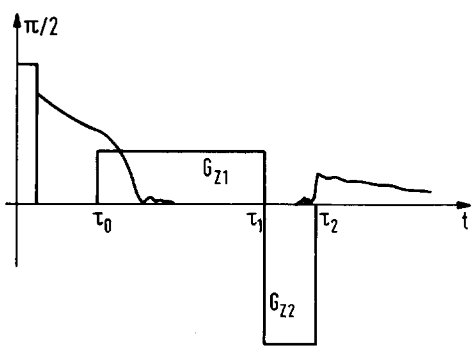

FIG. 10. Flow measurement by the gradient reversal method.

density, the eqn. (56) gives

$$U_D = K' \int \omega_{1r}(x,y,z+vt)\exp\left[-\frac{t}{T_2} + i(\gamma G_z z(t-\tau) + \tfrac{1}{2}\gamma G_z v_z(x,y)(t^2-\tau^2))\right] \mathrm{d}x\,\mathrm{d}y\,\mathrm{d}z. \quad (75)$$

The signal for a bulk sample with a non-uniform distribution of the flow velocities can be obtained by integration of eqn. (75) which gives a more complicated algebraical expression. The term $\exp(i\gamma G_z vt^2/2)$ gives rise to an increasing frequency as observed by Lent *et al.*[36]

The spin dephasing caused by the magnetic field gradient G_z can be removed without applying a π rf pulse by reversing the gradient after a certain period (Fig. 10). If the magnitude and the duration of the positive and negative gradient pulses fulfil the condition

$$F_z(t) = \gamma \int_{\tau_0}^{\tau_2} G_z(t)\,\mathrm{d}t \equiv 0 \quad (76)$$

then the signal dephasing is caused only by flow

$$f_z v_z = v_z \gamma \int_{\tau_0}^{\tau} G_z(t) t\,\mathrm{d}t = -\gamma G_{z1}(\tau_1 - \tau_0)(\tau_2 - \tau_0) v_2, \quad (77)$$

and the FID signal is

$$U_D = K' \int \mathrm{d}^3 r \omega_{1r}(x,y,z+v_2 t)\exp\left[-\frac{t}{T_2} - i\gamma G_{z1}(\tau-\tau_0)(\tau_2-\tau_0)v_z(x,y,z)\right]. \quad (78)$$

The treatment of the experiments which have more rf pulses applied together with the magnetic field gradient, and where B_1 is not uniform, is algebraically more complicated in the case of fluid flow.[14,16,47] However, our consideration will be limited to the situation where the rf field magnitude is uniform inside the solenoid of the length l. As before it is assumed that the rf field is completely uniform in the region $0 \leqslant z \leqslant l$ and zero outside of this region. In the spin–echo experiment where the excitation rf pulse is followed after a time τ by a rf pulse of length close to that of a π rf pulse, finite spatial extent of both pulses must be taken into account. If the magnetic field gradient is weak compared to the magnitude of the rf pulses then the time evolution operator for both rf pulses [eqns (19) and (23)] can be expressed in the same way as

$$U_{rf}(t) - \exp\left[i \sum_j I_{xj}\phi(t)\right] \quad (79)$$

with

$$\phi_j(t) = \gamma \int_0^t B_{1t}(\mathbf{r}_j(t'), t')\,\mathrm{d}t'. \quad (80)$$

Thus $\phi_j(t)$ depends on the spin location at time zero, $r_j(0)$, for the exciting pulse and at time τ for the π pulse, $r_j(\tau)$. Thus the effect of an rf field on the jth spin depends upon the location of the spin at time

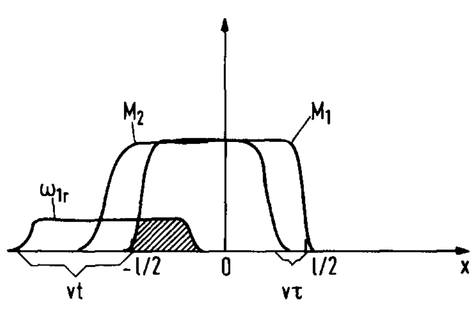

FIG. 11. The signals produced in the transmitter coil by the rf pulses, M_1 and M_2, and the signal in the receiving coil, ω_{1r}, seen from the frame moving with the spins.

of pulse application. The initial pulse excites the spins presently in the solenoid, while the π pulse inverts only those spins which have not left the solenoid before time τ. Substituting eqn. (79) in eqn. (25) then eqn. (32) becomes

$$U = \frac{\hbar^2\omega_0^2}{i_c}\sum_j \mathscr{B}_j \, Tr\, I_{xj} I_{xj}(t)\langle M_1(\mathbf{r}_j(0)) M_2(\mathbf{r}_j(\tau))\omega_{1r}(\mathbf{r}_j(t))\cos[\varphi_j(t)+\alpha_{1j}+\alpha_{2j}-\omega_o t]\rangle. \quad (81)$$

If one assumes a uniform spin density and neglects self-diffusion then eqn. (81) is transformed in the continuum limit into

$$U = \frac{\hbar^2\omega_0^2}{i_c}\mathscr{B}_o\, Tr\, I_x^2 \frac{N}{V}\exp\left(-\frac{t}{T_2}\right)\int d^3r\,\omega_{1r}(\mathbf{r}+\mathbf{v}t)M_1(\mathbf{r})M_2(\mathbf{r}+\mathbf{v}t)\cos[\mathbf{F}(t)(\mathbf{r}-\mathbf{r}_o)+\mathbf{f}(t)\mathbf{v}(\mathbf{r})+\alpha(\mathbf{r})-\omega_0 t]. \quad (82)$$

In the case when both transmitter and receiver coils are both solenoids the functions ω_{1r}, M_1 and M_2 have a similar form but are shifted in space with respect to each other (Fig. 11). The shift depends upon the direction of the flow, and therefore some precaution must be exercised when integrating eqn. (82). If the coil is symmetrical around the z-axis with uniform B_{1t} inside it and assuming that static G_{sz} as well as pulsed G_{pz} magnetic field gradients are applied along the z-axis then eqn. (82) leads to

$$U = \frac{\hbar^2\omega_0^2}{i_c}\mathscr{B}_0\, Tr\, I_x I_x(t)\frac{N}{V}\omega_{1r}M_1 M_2\int_{-l/2}^{l/2-v_z t}\cos\{\gamma G_{sz}(2\tau-t)(z-z_0)+v_2(x,y,z) \times [G_{sz}(\tau^2-\tfrac{1}{2}t^2)+G_{pz}\delta\Delta]-\omega_0 t\}\,dx\,dy\,dz \quad (83)$$

for flow along axis. If the flow is reversed then the integration in eqn. (83) goes from $-l/2+vt$ to $l/2$. Δ in eqn. (83) is the interspacing between two gradient pulses and δ is their width. For plug flow where the flow velocity is uniform eqn. (83) is

$$U \approx \exp\left(-\frac{t}{T_2}\right)\frac{\sin\left[\frac{\gamma}{2}G_{sz}(2\tau-t)(l-v_2 t)\right]}{\frac{\gamma}{2}G_{sz}l(2\tau-t)}\cos\{\gamma G_{sz}z_0(2\tau-t)\pm v_2\gamma[G_{sz}\tau(\tau-t)+G_{pz}\delta\Delta]\}, \quad (84)$$

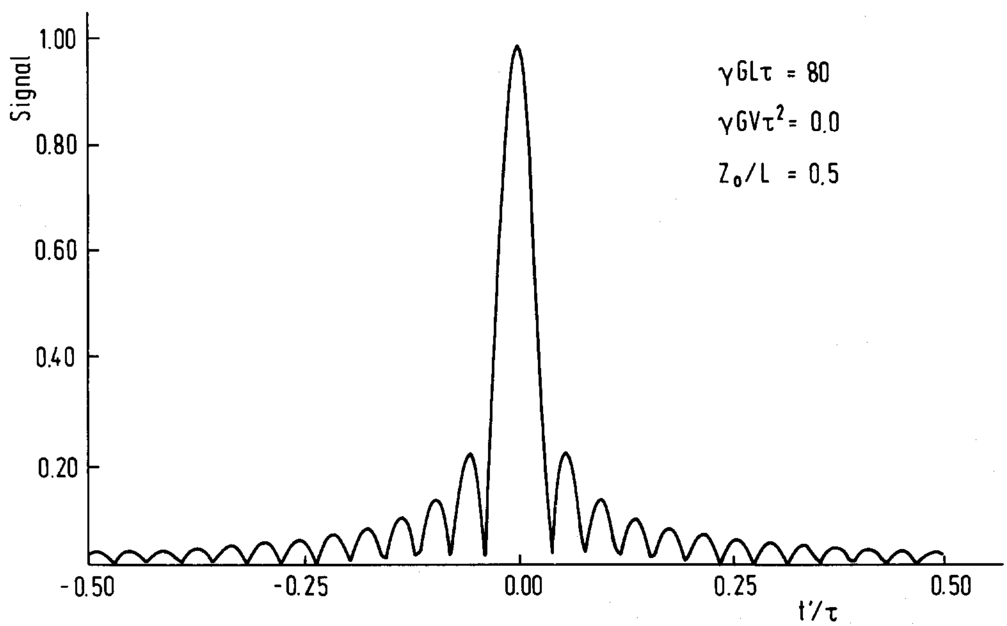

FIG. 12. The spin–echo signal from a stationary liquid.

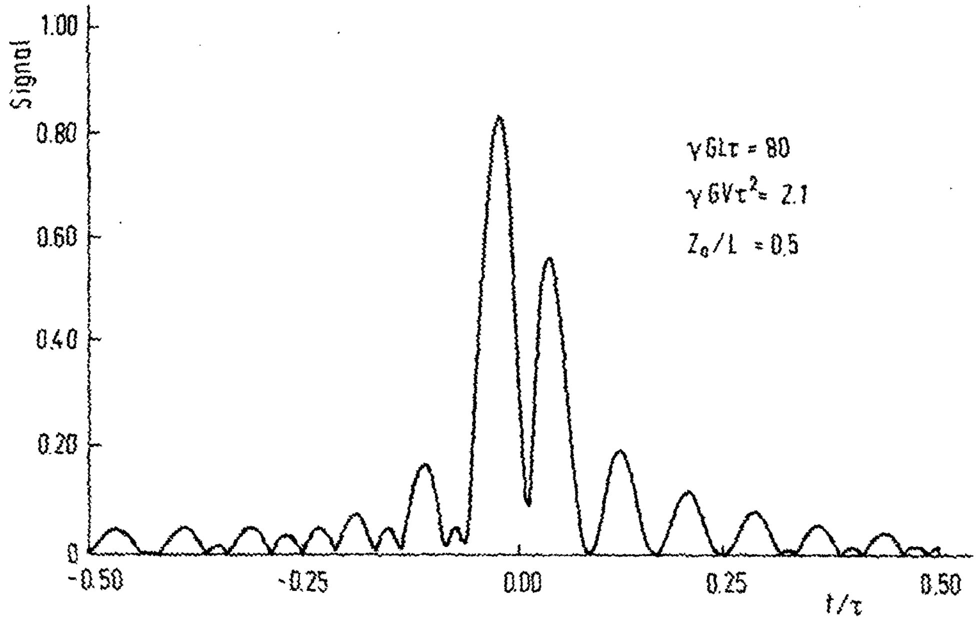

FIG. 13. The spin–echo signal from a flowing liquid.

where $+v$ means the flow along z-axis and $-v$ is flow in the opposite direction. This result is similar to that in Ref. (16) but certain differences appear since here the outflow of excited spins and the effect of the zero point of the gradient is taken into account. Thus, the spin–echo signal (84) depends also upon the position of the coil with respect to the zero plane $z = z_0$ of the magnetic field gradient. Figures 12 and 13 show the spin–echo signal after the sensitive demodulation, calculated from eqn. (84) if T_2 is neglected. The echo exhibits an asymmetry around $t = 2\tau$ similar to that observed in Ref. (16). The result for laminar flow will not be considered here but it can be calculated by inserting the proper velocity distribution in eqn. (83).

Parker[14] proposed a sequence which, for laminar flow, directly determines the velocity distribution function $\phi(v)$, representing the relative number of nuclear spins with a velocity v. This is a Carr–Purcell sequence[37] with the additional π pulse applied at the time of the echo maxima, $\pi/2-(\tau-\pi)_n$. In this case the spin–echo amplitude follows from eqn. (54). If the effects of rf inhomogenity, T_2 and self-diffusion are neglected, then the echo signal, at the point of refocusing when the condition $\mathbf{F}(t_n) = 0$ is fulfilled, becomes

$$U(t_n) \approx \int \cos(\mathbf{v}\mathbf{f}(t_m))\,\mathrm{d}^3r \equiv \int \phi(\mathbf{v})\cos(\mathbf{v}\mathbf{f}(t_m))\,\mathrm{d}^3v. \tag{85}$$

For a static magnetic field gradient eqn. (45) becomes

$$f(t_m) = t_m F(t_m) - \int_0^{t_m} F(t)\,\mathrm{d}t = \gamma G \frac{t_m}{n} t_m, \tag{86}$$

and the envelope of the echo maxima described by eqn. (85) is the Fourier transform of the velocity distribution function,

$$U \approx \int \phi(v)\cos(v\tau\gamma G t)\,\mathrm{d}v, \tag{87}$$

where $\tau = t_m/n$. This sequence has been used for the measurement of the blood flow velocity distribution in the human finger.[15] In order to compensate for rf inhomogeneity Garroway[17] has proposed the use of Hahn's spin–echo sequence, $\pi/2-(\tau-\pi/2_{90°})_n$, for the same problem.

4. FLOW IMAGING

4.1. *Imaging by Magnetization Transfer*

The first NMR imaging of the spatial profile of velocity in laminar flow in circular and rectangular pipes was obtained by Garroway.[17] The saturating $\pi/2$ rf pulse is followed by a $\pi/2$ rf excitation pulse after a time chosen to be greater than T_2^* but much less than the longitudinal relaxation time T_1. When the static magnetic field is applied in the z direction perpendicular to the direction of the fluid flow, then the fresh spins, unaffected by the first pulse enter the active region and the observed signal is proportional to

$$U \approx \tau \int \mathrm{d}z \int \mathrm{d}y \rho(y,z) v_x(y,z) \cos(\omega_0 t + \gamma G_z z t). \tag{88}$$

The same idea has been used in many imaging techniques[27,38-42,47,48] where more sophisticated sequences allow the imaging of a two-dimensional spatial velocity distribution. In the saturation recovery sequence the initial rf pulse saturates only the spins in a thin selected slice. During the subsequent waiting period, the spins partially recover by T_1 relaxation, but more importantly, they advance through the slice by a distance $l = v\tau$. Application of the selective detection rf pulse results in a signal that is stronger than it would be in the absence of flow. In the simplified case where the slice width l is assumed to be defined exactly the value of $\mathscr{B}$ at the time of the excitation rf pulse is given by

$$\mathscr{B}(y,z) = \mathscr{B}_0 \left[\frac{v\tau}{l} + \left(1 - \frac{v\tau}{l}\right)\left(1 - \exp\left(-\frac{\tau}{T_1}\right)\right)\right]. \tag{90}$$

Thus, the signal is induced by the fresh spins entering the selected slice as well as by the remaining spins which have partially recovered from the saturation. Thus, when imaging the body, vessels carrying rapidly flowing blood appear brighter than those containing slowly moving or stationary blood.

In the spin–echo sequences, the extent to which spins in the imaging slice are replaced by unlabelled spins, both between successive cycles and during the pulse interval must be considered in order to calculate the effect of flow on signal intensity.

Another version of the same technique involves the selective excitation of a number of parallel slices in successive time intervals and then monitoring of the magnetization transfer between them. Thus, the images obtained by this technique are a mixture of the velocity and density spatial distributions (if neglect T_1 and T_2), and discrimination between them is not always straightforward.

4.2. *Flow Phase Encoding*

The Fourier transformation of eqn. (56) with respect to **f** is

$$\mathscr{F}(\mathbf{r},\mathbf{v}) = A(\mathbf{r},\mathbf{v},T_2(\mathbf{r}))\exp[i(\mathbf{f}\mathbf{v}(\mathbf{r}) + \alpha(\mathbf{r}))] = R + iX. \tag{91}$$

Using an appropriate phase-cycled sequence[43-45] means that $\alpha(\mathbf{r})$ can be neglected and the velocity vector spatial distribution can be formally calculated from

$$\mathbf{f}\mathbf{v}(\mathbf{r}) = \tan^{-1}\left(\frac{X(\mathbf{r})}{R(\mathbf{r})}\right). \tag{92}$$

The gradient sequence determines which component of the phase factor **fv** will be accumulated in the time of the FID and, thus, it also determines which component of the velocity will be shown on the NMR image. This phase image is a pure image of the spatial distribution of the velocity without any additional mixing of other parameters like spin density or relaxation rates with the spatial distribution. The method can be interlaced[44] into a conventional NMR imaging method and the planar or even three dimensional distribution of the flow velocity can be visualized. The application of the flow phase encoding will be demonstrated in the next section by combining it with the spin warp imaging sequence.

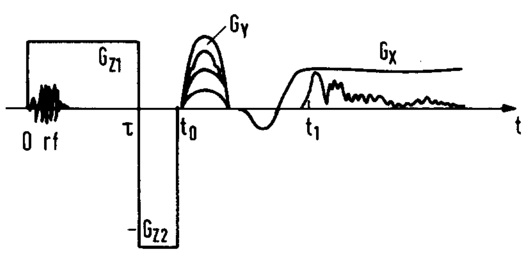

FIG. 14. The spin warp imaging sequence modified for the measurement of the flow phase encoding; measurement of the z-component of velocity.

4.3. *Flow Phase Encoding by the Spin Warp Technique*

The spin warp imaging sequence[26] is similar in principle to that proposed by Kumar *et al.*[24] called Fourier Zeugmatography. It uses spectrally shaped rf pulses in the presence of the field gradient to excite spins in a thin slice of the three dimensional sample and a sequence of gradient pulses in two perpendicular directions parallel to the selected slice in order to discriminate the planar distribution in the slice (Fig. 14). When used for flow phase encoding it is slightly modified. The modification concerns the gradient which brings about a phase shift related to the required component of the velocity vector. The sequence used for imaging the velocity component perpendicular to the selected plane is shown in Fig. 14. The only difference lies in the initial gradient pulse for which the positive part is prolonged and the negative part is amplified. If other gradients in the perpendicular directions are sufficiently weak then the dephasing $\mathbf{fv}$ is dominated by the component of the velocity perpendicular to the slice. Whenever velocity components parallel to the plane of the slice are imaged, a similar gradient but in the direction parallel to the slice should be applied, somewhere inside the original spin warp sequence (Fig. 15) and before the detection period has started.

Imaging of the velocity component perpendicular to the slice (z-direction) will now be considered in detail. The initial gradient consists of a positive part G_{z1}, from $t = 0$ to $t = \tau$, and of a negative part, $-G_{z2}$, from $t = \tau$ to $t = t_0$, such that

$$F_z = \gamma \int_0^{t_0} G_z(t)\,\mathrm{d}t \equiv 0 \tag{93}$$

and that

$$f_z = \gamma \int_0^{t_0} tG_z(t)\,\mathrm{d}t = -\gamma G_{1z}\tau t_0 \tag{94}$$

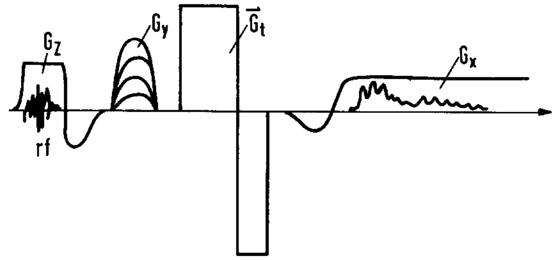

FIG. 15. The spin warp sequence imaging sequence modified for measuring of an arbitrary component of velocity, $\mathbf{v}_t$.

according to (77). It is approximated that

$$f_x = f_y \approx 0 \tag{95}$$

since f_z is dominant. The spin phase twist is introduced by adding a y-field gradient, after the selective excitation and before the readout. In each successive sequence, G_y has the same slope but its amplitude changes by equal steps from zero to its maximal value so that

$$F_y = ng_y \tag{96}$$

with

$$g_y = \gamma \int_0^t G_y(t')\,\mathrm{d}t'. \tag{97}$$

The gradient G_x (Fig. 14) is applied in the readout period. Thus, the observed signal is the function of two parameters, t and n, and is given as

$$U_{\mathrm{D}} = K \int \rho_{\mathrm{eff}}(x,y,z) M_1(z-z_0) \exp[i(\gamma G_x(x-x_0)(t-t_1) + g_y n(y-y_0) + f_z v_z(x,y,z) + \alpha_1(z-z_0))]\,\mathrm{d}x\,\mathrm{d}y\,\mathrm{d}z. \tag{98}$$

The factor $M_1(z-z_0)$ and the phase shift $\alpha_1(z-z_0)$ are determined by the rf field and gradient G_{z1}. Their approximative calculation is given in the Appendix. In fact M_1 which determines the slice size is non-zero only in the thin region around $z = z_0$.

The Fourier transformation of eqn. (98) with respect to time t

$$\mathscr{F}'_1(\omega_x, n) = \frac{1}{\tau_0} \int_0^{\tau_0} U_{\mathrm{D}}(t,n) \exp[i\omega_x t]\,\mathrm{d}t \tag{99}$$

gives the complex function which depends upon n and the coordinate x, and also upon the position of selected slice $z = z_0$

$$\mathscr{F}_1(x, z_0, n) = K \int \rho_{\mathrm{eff}}(x,y,z) M_1(z-z_0) M_2\left(\frac{\omega_x}{\gamma G_x} - x + \omega_0\right) \exp[i(g_y n(y-y_0) + \alpha_1 + \alpha_2 + f_z v_z(x,y,z)]\,\mathrm{d}x\,\mathrm{d}y\,\mathrm{d}z. \tag{100}$$

In eqn. (100)

$$M_2(a) = \sqrt{A^2(a) + D^2(a)} \qquad \text{and} \qquad \alpha_2(a) = \tan^{-1}\left(\frac{D(a)}{A(a)}\right), \tag{101}$$

where the functions A and D depend on τ_0, the time interval used for data collection. If τ_0 is longer than the relaxation time T_2 then we get the absorption signal

$$A(a) = \frac{T_2/\tau_0}{1 + (\gamma a T_2 G_x)^2} \tag{102}$$

and the dispersion signal as

$$D(a) = \frac{T_2^2 \gamma a G_x/\tau_0}{1 + (\gamma a T_2 G_x)^2}. \tag{103}$$

But if τ_0 is shorter than the relaxation time T_2, these functions are

$$A(a) = \frac{\sin \gamma a G_x \tau_0}{\gamma a G_x \tau_0} \tag{104}$$

and

$$D(a) = \frac{1 - \cos \gamma a G_x \tau_0}{\gamma a G_x \tau_0}. \tag{105}$$

In the last case M_2 and α_2 have the simple forms

$$M_2(a) = \frac{\sin\left(\frac{\gamma a G_x \tau_0}{2}\right)}{\frac{\gamma a G_x \tau_0}{2}} \tag{106}$$

and

$$\alpha_2(a) = -\frac{\gamma a G_x \tau_0}{2}. \tag{107}$$

After Fourier transformation with respect to the parameter n

$$\mathscr{F}_2(x, z, \omega_y) = \frac{2}{N}\sum_{n=0}^{N} \mathscr{F}_1(x, z, n)\exp[-in\omega_y] \tag{108}$$

one gets a result which is the function of three spatial coordinates

$$\mathscr{F}(x, y, z) = K\int \rho_{\text{eff}}(x, y, z) M_1(z-z_0) M_2\left(\frac{\omega_x}{\gamma G_x} - x + x_0\right) M_3\left(\frac{\omega_y}{g_y} - y + y_0\right)$$
$$\exp[i(f_z v_z(x, y, z) + \alpha_1 + \alpha_2 + \alpha_3)]\,\mathrm{d}x\,\mathrm{d}y\,\mathrm{d}z \tag{109}$$

with

$$M_3(a) = \frac{\sin g_y a(N/2)}{\sin g_y a(N/2)} \tag{110}$$

and

$$\alpha_3(a) = (N+1)g_y a/2. \tag{111}$$

N is the number of steps for G_y. The functions $M_1(z-z_0)$, $M_2(\omega_x/\gamma G_x - x + x_0)$ and $M_3(\omega_y/g_y - y + y_0)$ can be approximated as delta functions and then the result of integration of eqn. (109) is

$$\mathscr{F}(\mathbf{r}) = \rho_{\text{eff}}\left(\frac{\omega_x}{\gamma G_x} + x_0, \frac{\omega_y}{g_y} + y_0, z_0\right)\exp\left[if_z v_z\left(\frac{\omega_x}{\gamma G_x} + x_0, \frac{\omega_y}{g_y} + y_0, z_0\right)\right] \tag{112}$$

whose magnitude is the planar spin density distribution in the planar slice, while the phase is proportional to the planar distribution of the z-component of the velocity

$$v_z = -\frac{1}{\gamma G_{z1}\tau_0 t_0}\tan^{-1}\left[\frac{Im\mathscr{F}(\mathbf{r})}{Re\mathscr{F}(\mathbf{r})}\right]. \tag{113}$$

Figure 16 shows the expected image of the spin density and flow velocity in the human body.

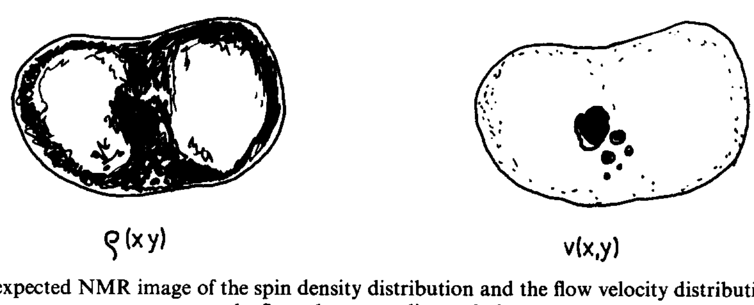

FIG. 16. The expected NMR image of the spin density distribution and the flow velocity distribution obtained by the flow phase encoding technique.

APPENDIX

In the selective excitation experiment only part of the spin magnetization interacts strongly with the rf pulse. This can be achieved by applying a linear magnetic field gradient over the sample, for example, along the z-axis, simultaneously with the excitation rf pulse. Thus only the spins in the thin slice in the x–y plane are at exact resonance and capable of being rotated by an rf pulse. Spins on either side of this plane will be progressively less affected the further they are from this isocromatic plane. Using the density matrix approach, an exact solution can be found only in the case when the amplitude of the rf field and the amplitude of the magnetic field gradient are constant during their simultaneous application. In this case, the transformation into the frame which rotates with ω_0 around the z-axis can be achieved by separating the time evolution operator into

$$U(t) = U_Z(t)U_{\mathrm{rf}+G}(t) \tag{A1}$$

where U_Z has its usual meaning but

$$U_{\mathrm{rf}+G}(t) = \exp\left[i\sum_j (\Delta_j I_{zj} + \omega_{1t} I_{xj})t\right], \tag{A2}$$

with

$$\Delta_j = \gamma G_z(z_j - z_0). \tag{A3}$$

The Hamiltonian in the commulant of eqn. (A2) is time independent and there is no time ordering as in eqn. (19). Thus, $U_{\mathrm{rf}+G}$ transforms the longitudinal magnetization to give

$$U_{\mathrm{rf}+G} I_z U_{\mathrm{rf}+G}^{-1} = \sum_j \left[I_{xj}\frac{2\omega_{1t}\Delta_j}{\omega_{1t}^2+\Delta_j^2}\sin\left(\tfrac{1}{2}\sqrt{\omega_{1t}^2+\Delta_j^2}\,\tau\right) - I_{yj}\frac{\omega_1}{\sqrt{\omega_{1t}^2+\Delta_j^2}}\sin\left(\sqrt{\omega_{1t}^2+\Delta_j^2}\,\tau\right) + I_z\left(1 - 2\frac{\omega_{1t}}{\sqrt{\omega_{1t}^2+\Delta_j^2}}\sin\left(\tfrac{1}{2}\sqrt{\omega_{1t}^2+\Delta_j^2}\,\tau\right)\right)\right]. \tag{A4}$$

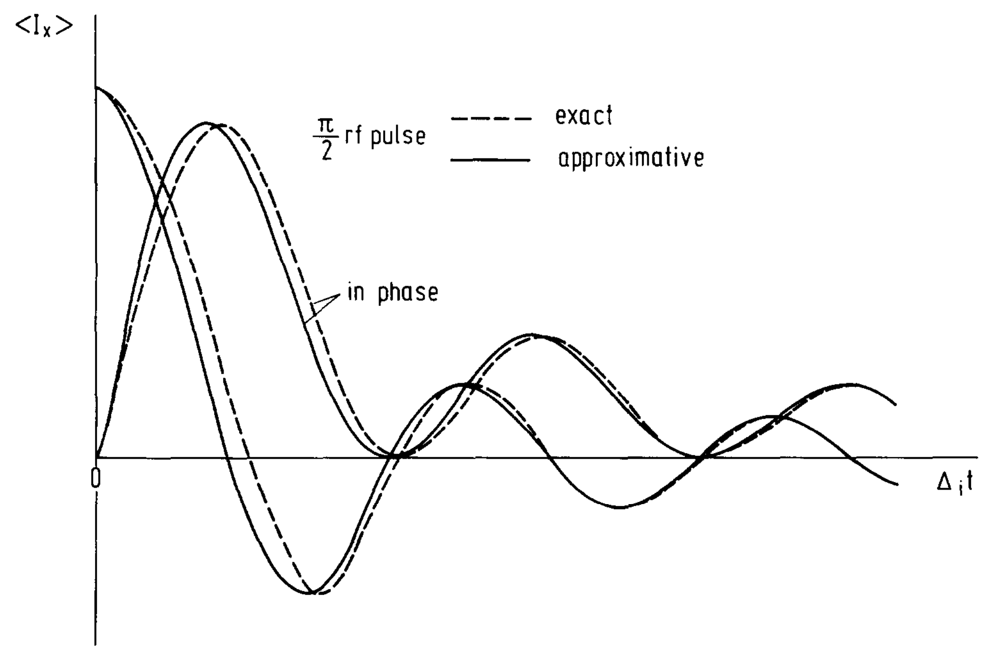

FIG. 17. The spatial distribution of the transverse magnetization induced by $\pi/2$ pulse: __ __ __ exact calculation and ______ calculation by the zeroth order term of the Magnus expansion.

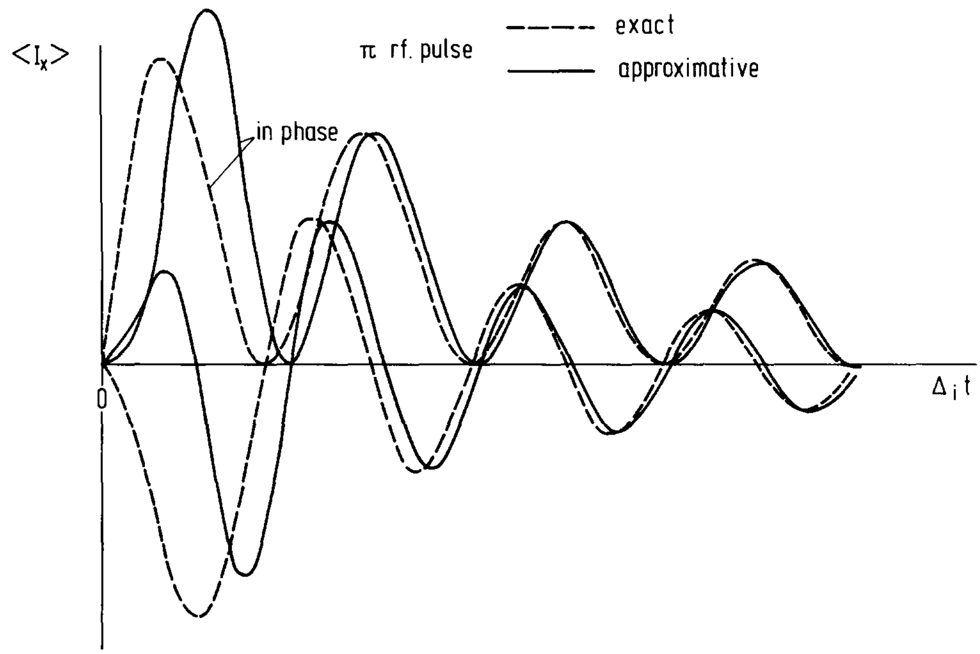

FIG. 18. The spatial distribution of the transverse magnetization induced by π pulse: __ __ __ exact calculation and ______ calculation by the zeroth order term of the Magnus expansion.

The x and y components of the magnetization for a $\pi/2$ rf pulse (Fig. 17) and for a π rf pulse (Fig. 18) are evaluated from eqn. (A4).

However, in general the selective rf pulse is not rectangular but is modulated with a desired spectral distribution. In such cases the evaluation of eqn. (A4) is not so straightforward because the presence of the time ordering necessitates the use of approximative methods. In the general case, when both B_{1t} and G_z depend upon time, we can make the transformation into a non-uniformly rotating frame as before

$$U(t) = U_Z(t)U_G(t)U_{rf}(t), \tag{A5}$$

where all terms have the usual meaning as in eqns (18), (21) and (23). The time evolution operator requires time ordering and here we shall expand it into a Magnus series,[31] and by taking into account only the zeroth approximation of the expansion

$$U_{rf}^{(0)}(t) = \exp(iF_0(t)) = \exp\left[i\sum_j a_j(t)I_{xj}+b_j(t)I_{yj}\right] \tag{A6}$$

with

$$a_j(t) = \int_0^\tau \omega_{1t}(t)\cos\varphi_j(t)\,\mathrm{d}t \tag{A7}$$

$$b_j(t) = -\int_0^\tau \omega_{1t}(t)\sin\varphi_j(t)\,\mathrm{d}t, \tag{A8}$$

and

$$\varphi_j(t) = \gamma\int_0^t \mathrm{G}_z(t')(z(t')-z_0)\,\mathrm{d}t'. \tag{A9}$$

Using this we can calculate

$$U_{\rm rf}^{(0)} I_z U_{\rm rf}^{(0)-1} = \sum_j A_j(t) I_{xj} + B_j(t) I_{yj} + C_j(t) I_{zj} \tag{A10}$$

with

$$A_j(t) = \frac{b_j}{\sqrt{a_j^2+b_j^2}} \sin\sqrt{a_j^2+b_j^2} \tag{A11}$$

$$B_j(t) = -\frac{a_j}{\sqrt{a_j^2+b_j^2}} \sin\sqrt{a_j^2+b_j^2} \tag{A12}$$

and

$$C_j(t) = \cos\sqrt{a_j^2+b_j^2}. \tag{A13}$$

At the end of the rf pulse at $t = \tau$ the magnetization is rotating as

$$U_G U_{\rm rf}^{(0)} I_z U_{\rm rf}^{(0)-1} U_G^{-1} = \sum_j [A_j(\tau)\cos\varphi_j(t) - B_j(\tau)\sin\varphi_j(\tau)] I_{xj} + [B_j(\tau)\cos\varphi_j(\tau) + A_j(\tau)\sin\varphi_j(\tau)] I_{yj} + C_j(\tau) I_{zj}. \tag{A14}$$

For a rectangular rf pulse and a static gradient the equations (A7), (A8) and (A11)–(A13) become

$$\begin{aligned} a_j &= \omega_{1t}\sin\Delta_j t \\ b_j &= \omega_{1t}(1-\cos\Delta_j t) \end{aligned} \tag{A15}$$

and

$$\begin{aligned} A_j &= -\sin\left[\frac{2\omega_{1t}}{\Delta_j}\sin\frac{\Delta_j\tau}{2}\right]\sin\frac{\Delta_j\tau}{2} \\ B_j &= -\sin\left[\frac{2\omega_{1t}}{\Delta_j}\sin\frac{\Delta_j\tau}{2}\right]\cos\frac{\Delta_j\tau}{2} \\ C_j &= \cos\left(\frac{2\omega_{1t}}{\Delta_j}\sin\frac{\Delta_j\tau}{2}\right). \end{aligned} \tag{A16}$$

Thus the magnetization given by eqn. (A14) after the excitation behaves as

$$U_G U_{\rm rf}^{(0)} I_z U_{\rm rf}^{(0)-1} U_G^{-1} = \sum_j \left[\sin\left(\frac{2\omega_{1t}}{\Delta_j}\sin\frac{\Delta_j\tau}{2}\right)\left(I_{xj}\cos\frac{\Delta_j\tau}{2} - I_{yj}\sin\frac{\Delta_j\tau}{2}\right) + I_{zj}\cos\left(\frac{2\omega_{1t}}{\Delta_j}\sin\frac{\Delta_j\tau}{2}\right)\right]. \tag{A17}$$

Figures 17 and 18 both show the transverse component of the magnetization after selective excitation calculated exactly and by the zeroth order approximation of the Magnus expansion. There is only a small difference in the results of the two calculations for the $\pi/2$ rf pulse, but this difference increases significantly when the pulse length is longer than a π rf pulse.

REFERENCES

1. N. BLOMBERGEN, E. M. PURCELL and R. V. POUND, *Phys. Rev.* **73**, 679 (1948).
2. E. L. HAIN, *Phys. Rev.* **80**, 580 (1950).
3. H. C. TORREY, *Phys. Rev.* **76**, 1059 (1949).
4. G. SURYAN, *Proc. Indian Acad. Sci., Sect.* **A33**, 107 (1951).
5. P. KUSCH, *Phys. Rev.* **101**, 627 (1956).
6. J. P. BARRAT and J. W. WINTER, *J. Physique* **17**, 833 (1956).
7. A. Z. HRYNKIEWICZ and T. WALUGA, *Acta Phys. Pol.* **16**, 381 (1957).
8. E. O. STEJSKAL, *J. Chem. Phys.* **43**, 3597 (1965).
9. A. I. ZHERNOVOI and G. D. LATYSHEV, *NMR in a Flowing Liquid*, Plenum, New York (1965).
10. L. R. HIRSHEL and L. F. LIBELO, *J. App. Phys.* **32**, 1404 (1961) and **33**, 1859 (1962).
11. W. F. GENTHE, W. R. VARDEN HEYDEN, H. H. BATTOCLETTI, W. S. MCCORMICK and H. M. SNOWBALL, *Instrum. Technol.* **15**, 53 (1968).

12. J. R. SINGER, *Science* **130**, 1652 (1959).
13. J. R. SINGER, *IRE Trans. Med. Electron.* **7**, 23 (1960).
14. K. J. PACKER, *Mol. Phys.* **17**, 355 (1969).
15. T. GROVER and J. R. SINGER, *J. App. Phys.* **42**, 938 (1971).
16. R. J. HAYWOOD, K. J. PACKER and D. J. TOMLINSON, *Mol. Phys.* **23**, 1083 (1972).
17. A. N. GARROWAY, *J. Phys.* **D7**, L159 (1974).
18. P. A. DE JAGER and M. A. HEMMINGA, *Rev. Sci. Instr.* **49**, 1217 (1978).
19. B. BARBÊ, M. LEDUC and F. LALOË, *J. Physique* **35**, 699, 935 (1974).
20. R. GABILARD, *Phys. Rev.* **85**, 694 (1952).
21. P. C. LAUTERBUR, *Nature* **242**, 190 (1973).
22. A. N. GARROWAY, P. K. GRANNEL and P. J. MANSFIELD, *J. Phys.* **C2**, L457 (1974).
24. A. KUMAR, D. WELTI and R. R. ERNST, *J. Mag. Res.* **18**, 69 (1975).
25. R. DAMADIAN, M. GOLDSMITH and L. MINKOF, *Physiol. Chem. Phys.* **9**, 97 (1977).
26. W. A. EDELSTEIN, J. M. S. HUTCHINSON, G. JOHNSON and T. W. REDPATH, *Phys. Med. Biol.* **25**, 751 (1980).
27. L. KAUFMAN, L. E. CROOKS and A. R. MARGULIS, Eds., *Nuclear Magnetic Resonance Imaging in Medicine*, Igaku-Shoiu Medical Pub., New York (1981).
28. P. MANSFIELD and P. G. MORRIS, *NMR Imaging in Biomedicine*, Suppl. 2, *Advances in Magnetic Resonance*, Academic Press (1982).
29. D. McDONALD, *Blood Flow in Arteries* 2nd ed., Williams & Wilkins, Baltimore (1974).
30. D. F. HOULT and R. E. RICHARDS, *J. Mag. Res.* **24**, 71 (1976).
31. W. A. B. EVANS, *Annals of Physics* **48**, 72 (1968).
32. R. KUBO, In: *Lectures in Theoretical Physics*, Vol. 1, Eds. W. E. BRITTIN and L. G. DURHAM, p. 181, Interscience Publishers Ltd., London (1959).
33. J. STEPIŠNIK, *Physica* **104B**, 350 (1981).
34. D. W. JONES and T. F. CHILD, *NMR in Flowing Systems*, *Advances in Magnetic Resonance*, Vol. 8, Academic Press (1976).
35. J. STEPIŠNIK, *J. Physique* **39**, 689 (1978).
36. A. H. LENT, H. N. YEUNG, W. S. HINSHAW, D. M. KRAMER and L. R. BALKANYI, *Mag. Res. Med.* **1** (1984).
37. H. Y. CARR and F. M. PURCELL, *Phys. Rev.* **94**, 630 (1954).
38. J. P. GRANT and C. BACK, *Med. Phys.* **9(2)**, 188 (1982).
39. L. E. CROOKS, C. M. MOLLS, P. L. DAVIS, M. BRANDT-ZAWADSKI, J. HOENNINGER, A. ARAKAWA, J. WATTS and L. KAUFMAN, *Radiology* **144**, 843 (1982).
40. C. R. GEORGE, J. GORDON, WM. J. MACINTYRE, R. J. LORIG, D. M. KRAMER, R. T. GO, Y. NOSE and T. F. MEANCY, *Mag. Res. Med.* **1**, 154 (1984).
41. D. P. LALLEMAND, G. E. WESBEY, C. A. GOODING and R. C. BRASCH, *Mag. Res. Med.* **1**, 285 (1984).
42. A. BONMARTIN, A. BRIQUET, J. DELMAN, D. GRAVERON-DEMILLY, C. LAPRAY, J. L. LEFEVRE and J. J. MALLET, *Mag. Res. Med.* **1**, 109 (1984).
43. J. STEPIŠNIK, Paper presented at the 6th EENC Conference (1982).
44. P. R. MORAN, *Mag. Res. Imaging* **1**, 197 (1983).
45. A. CONSTANTINESCO, J. J. MALLET, A. BONMARTIN, C. LALLOT and A. BRIQUET, *Mag. Res. Imaging* **2**, 335 (1984).
46. A. M. HEMMINGA, P. A. DE JAGER and A. SONNEVELD, *J. Mag. Res.* **27**, 359 (1977) and **37**, 1 (1980).
47. K. R. THILBORN, J. C. WATERTON and G. K. RADDA, *J. Mag. Res.* **45**, 188 (1981).
48. J. H. BATTOCLETTI and R. E. HALBACH, *J. Mag. Res.* **52**, 500 (1983).